RESEARCH ARTICLE

Comparative transcriptomics of sclerotia and mycelia of *Rhizoctonia solani* AG2-2IIIB

M.E. Haque[1], M.S Parvin[2,3*]

Haque ME, Parvin MS. Comparative transcriptomics of sclerotia and mycelia of *Rhizoctonia solani* AG2-2IIIB. AGBIR. 2021;37(2):116-123.

The fungus *Rhizoctonia solani* AG2-2IIIB causes root and crown rot on sugar beet, an important disease worldwide. This necrotrophic pathogen overwinters in crop residues and soil as sclerotia. This resting form germinates under favorable condition to infective hyphae that initiate the infections to sugar beet. Despite the global importance of this deadly soil-borne pathogen, the molecular basis of sclerotia development is poorly understood. Besides, *R. solani* AG2-2IIIB, hardly produces basidiospores; therefore, understanding the molecular mechanism of sclerotia formation is crucial for crop disease control. In the current investigation, RNA-seq (next generation sequencing, NGS) was persuaded via DNA nanoballs (DNB) to understand the transcriptome dynamics of mycelia and sclerotia. A total of 4185 differentially expressed genes (DEGs) and 6820 non- differentially expressed genes (DEGs) were identified between sclerotia and mycelia stage. Among the highly upregulated genes that encode enzymes or proteins were included cytochrome c oxidase, cytochrome c peroxidase, superoxide dismutase (SOD), cytochrome P450, oxidoreductase, signal peptidase complex, apoptosis-inducing factors, NADPH oxidase, chitinases, serine/threonine kinases, programmed cell death proteins, Transcription elongation factor 1-beta, subtilisin-like protease 8, poly-ubiquitin-A, glutathione peroxidase, phosphatidylserine decarboxylases, and hypothetical proteins identified in the transcriptome of sclerotia and mycelia. Moreover, gene ontology (GO) and kyoto encyclopedia of genes and genomes (KEGG) analyses showed that these DEGs were enriched in diverse categories, including oxidoreductase activity, carbohydrate metabolic process, and oxidation-reduction processes.

Key Words: *RNA-seq; Sclerotia; Mycelia; R. solani AG2-2IIIB*

INTRODUCTION

The basidiomycetes fungus *R. solani Kühn* (teleomorph Thanatephorus cucumeris Donk) is a cosmopolitan, devastating soil-borne pathogen causing consistent economic losses in a wide range of cereals, tubers, oilseed crops, and vegetables as well as ornamental plants and forest trees [1-5]. It is known to have a necrotrophic lifestyle which has a variety of disease name based on crop plants; for instance, rice sheath blight, bare patch on cereals, black scurf on potatoes, sugar beet seedling crown and root rot as well as damping-off, root and stem rot on Soybean. Till today, 14 anastomosis groups (AG) have reported in *R. solani*, AG-1 to AG-13, and AG-BI (bridging isolate), which has two subgroups, AG2-2IIIB and AG2-2 IV [6-8]. Several studies with diseased sugar beets have shown the presence of AG-1, AG 2-1, AG2-2, AG-3, AG-4, and AG-5 [9]. Nevertheless, the most aggressive form is AG2-2IIIB which infects seedlings as well as older sugar beets [10]. It is known as facultative saprophyte, but its pathogenesis is poorly understood. It occasionally forms sexual spores, although it does not produce any asexual spores. It can survive 8-10 years via forming sclerotia that can remain in soil or crop residues [11]. The primary form of the pathogen in nature is mycelia [1]. Sclerotia development initiated with increased phenol oxidase activity as known from AG1-IA [12]. Several abiotic cues are involved prior to the development of sclerotia, such as nutrient shortfall, temperature, pH, light intensity, erratic aeration, and the presence of antioxidants [13-16]. However, there is not sufficient information about the molecular mechanisms involved in *R. solani* AG2-2IIIB sclerotia transformation, especially, changes in gene expression at the transcriptome level. RNA-seq (next-generation sequencing-NGS) which is a powerful technology to understand genome-wide differential gene expression in a biological system. This covers coding sequences, gene function, alternate splicing, and metabolic pathways [17,18]. Previously, transcriptome analysis of *R. solani* AG1-IA showed molecular mechanisms of sclerotia development in maize (*Zea mays*) and rice (*Oryza sativa*) sheath blight [18,19]. Kwon et al. [19] also demonstrated proteomics profile of sclerotia development at different time points. As far as we are concerned, this is the first transcriptome analysis of sclerotium formation of *R. solani* AG2-2IIIB via DNA nanoballs (DNBs) platform. In this project, 6 samples were sequenced (3-sclerotial and 3-mycelial samples) and de novo assembled the *R. solani* AG2-2IIIB transcriptome using draft genome of *R. solani* AG2-2IIIB (https://www.ebi.ac.uk/ena/data/view/GCA_001286725.1), averagely generating about 10.22 Gb bases per sample. The average mapping ratio to the draft genome of *Rhizoctonia solani* AG2-2IIIB was 51%, the average mapping ratio with gene was 50.39%; 12,077 genes were identified in which 10,851 of them are known genes and 1,226 of them were novel genes. 6,063 novel transcripts were identified in which 2,978 of them were previously unknown splicing event for known genes, 1,226 of them were novel coding transcripts without any known features, and the remaining 1,859 were long noncoding RNA.

MATERIALS AND METHODS

RNA extraction and Quality Control (QC)

The same isolate (MN128569) of *R. solani* AG2-2IIIB was grown in the amended clarified V8 (ACV8) media (100x15 mm, Petri Dish, VWR) at 28°C in the dark for three weeks. Sclerotia and mycelial biomass were separately collected 21 days after. Sclerotia were picked with sterilized forceps, while mycelial biomass was collected using scalpel separately (1.5 ml Eppendorf tube) from 6-independent culture plate, and freeze dried to a completely dry form (1600 MiniG-SPEX Sample Prep). Total RNA was extracted from mycelia and sclerotia using a RNeasy Mini Kit (Cat No./ID: 74904, Oiagen, USA) according to the manufacturer's instructions. Extracted RNA was then treated with DNase I to remove any genomic DNA, and purified using a RNeasy MinElute Cleanup Kit (Cat No./ID: 74204, Oiagen USA). RNA quality and yield were measured using gel electrophoresis and spectrophotometry (NanoDropTM 2000/2000c, Thermo Fisher Scientific, USA). We used Agilent 2100 Bio analyzer (Agilent RNA 6000 Nano Kit) to do the total RNA sample QC: RNA concentration, RNA Integrity Number (RIN) value above 8.0 was considered, 28S/18S and the fragment length distribution. For sclerotia and mycelial samples, NanoDropTM was used to measure the purity of the RNA samples. Three biological replicates for each sample were used to prepare libraries [18].

Library construction

The first step in the workflow involved purifying the poly-A containing mRNA molecules using poly-T oligo attached magnetic beads. Following purification, the mRNA was fragmented into small pieces using divalent cations under elevated temperature. The cleaved RNA fragments were copied into first strand cDNA using reverse transcriptase and random primers. This was followed by second strand cDNA synthesis using DNA Polymerase I and RNase H. These cDNA fragments then had the addition of a single 'A' base

[1]*University of North Dakota, Grand Forks, USA ;*[2]*Department of Natural Science, Leibniz University Hannover, Germany;*[3]*Plant Breeding Division, Bangladesh Agricultural Research Institute, Gazipur, Bangladesh*

Correspondence: *M.S Parvin, Department of Natural Science, Leibniz University, Hannover, Germany, E-mail: shanaj.p@bari.gov.bd*

Received: *March 01, 2021,* **Accepted:** *March 15, 2021,* **Published:** *March 22, 2021*

and subsequent ligation of the adapter. The products were then purified and enriched with PCR amplification. We then quantified the PCR yield by Qubit and pooled samples together to make a single strand DNA circle (ssDNA circle), which gave the final library. DNA nanoballs (DNBs) were generated with the ssDNA circle by rolling circle replication (RCR) to enlarge the fluorescent signals at the sequencing process.

The DNBs were loaded into the patterned nanoarrays and pair-end reads of 100 bp were read through on the DNBseq platform for the following data analysis study. For this step, the DNBseq platform combined the DNA nanoball-based nanoarrays and stepwise sequencing using Combinational Probe-Anchor Synthesis Sequencing Method https://www.bgi.com/us/sequencing-services/rna-sequencing-solutions/transcriptome-sequencing/).

Bioinformatics

Firstly, the low-quality reads were filtered (More than 20% of the bases qualities are lower than 10), reads with adaptors and reads with unknown bases (N bases more than 5%) to get the clean reads. Subsequently, those clean reads were mapped onto reference genome (GCA_001286725.1_AG22IIIB), followed with novel gene prediction, single nucleotide polymorphism (SNP) & insertion and deletion (INDEL) calling and gene-splicing detection. Finally, DEGs (differentially expressed genes) were identified between samples, and performed clustering analysis and functional annotations.

Sequencing reads filtering

Software SOAPnuke (version: v1.5.2 parameters: -l 15 -q 0.5 -n 0.1) was used to filter reads, as followed: 1) Adaptors were removed from the reads; 2) Reads were removed in which unknown bases(N) were more than 10%; 3) low quality reads were remove (the low quality read as the percentage of base which quality was lesser than 15 and greater than 50% in a read). After filtering, the remaining reads were called "Clean Reads" and stored in FASTQ format used for downstream analyses [20].

Genome mapping

Hierarchical indexing for spliced alignment of transcripts (HISAT2) were used to do the mapping step. The bam files were provided for the genome mapping results. Integrative Genomics Viewer (IGV) tool was used to review the mapping result. IGV supported importing multiple samples for comparison and showed the distribution of reads in the exon, intron, UTR, intergenic areas based on the annotation result. HISAT2 which was much faster, sensitive and high accuracy analysis software [21].

Novel transcript prediction

StringTie [Version: v1.0.4] was used to reconstruct transcripts, and used Cuffcompare‖Cufflinks [Version: v2.2.1] tools) to compare reconstructed transcripts to reference annotation, after that, we select 'u' (Unknown, intergenic transcript) ,'i' (A transfrag falling entirely within a reference intron), 'o' (Generic exonic overlap with a reference transcript),'j' (Potentially novel isoform/fragment: at least one splice junction is shared with a reference transcript) class code types as novel transcripts. And then, we use CPC [Version: v0.9-r2] to predict coding potential of novel transcripts, then the coding novel transcripts were merged with reference transcripts to get a complete reference, and downstream analysis was based on this reference. StringTie was much faster and accurate software for transcriptome assembly, compared to Cufflinks software [21-25].

SNP and INDEL detection

Genome mapping result was used via GATK to call SNP and INDEL for each sample. After filtered out the unreliable sites, we obtained the final SNP and INDEL in VCF format [26].

Gene expression analysis

Clean reads were mapped to reference using Bowtie2 [Version: v2.2.5], and then the gene expression level was calculated with RSEM [Version: v1.2.12]. RSEM was a software package for estimating gene and isoform expression levels from RNA-Seq data. Pearson correlation was calculated between all samples using cor, and the diagrams were drawn with ggplot2 with functions of R.

Gene expression cluster analysis

The clustering results were displayed with javaTreeview using cluster [Version: v3.0, Parameters: -g 7 -e 7 -m a] software to analyze the expression genes and sample scheme at the same time by using the Euclidean distance matrix as the matrix formula [27,28].

DEG detection

DEGs were detected with PossionDis (Parameters: Fold Change ≥ 2.00 and FDR ≤ 0.001). It is based on the poisson distribution as described Audic S [29].

Hierarchical clustering analysis of DEG

Hierarchical clustering was performed for DEGs using pheatmap, a function of R. For cluster more than two groups, we perform the intersection and union DEGs between them, respectively.

Gene ontology analysis of DEG

With the GO annotation result, we classified DEGs according to official classification, and we also performed GO functional enrichment using phyper, a function of R. The pvalue was calculated using the hypergeometric test as followed:

$$P = 1 - \sum_{i=0}^{m-1} \binom{M}{i}\binom{N-M}{n-i} / \binom{N}{n}$$

Later, we calculated false discovery rate (FDR) for each pvalue, in general, the terms which FDR not larger than 0.01 were defined as significantly enriched.

Pathway analysis of DEG

With the KEGG annotation result, we classified DEGs according to official classification, and we also made pathway functional enrichment using phyper, a function of R. The pvalue calculating formula in hypergeometric test was:

$$P = 1 - \sum_{i=0}^{m-1} \binom{M}{i}\binom{N-M}{n-i} / \binom{N}{n}$$

Later, we calculated false discovery rate (FDR) for each pvalue, in general, the terms which FDR not larger than 0.01 were defined as significant enriched.

PPI analysis of DEG

We used DIAMOND (Version: v0.8.31) to map the DEGs to the STRING (Version: v10) database to obtain the interaction between DEG -encoded proteins using homology with known proteins. We selected the top 100 interaction networks to draw the picture, for the entire interaction result we provided an input file that can be imported directly into Cytoscape for network analysis. Cytoscape was software for complex network analysis and visualization [30].

Fungal pathogenic gene prediction

BLAST (Version: v2.5.0) or DIAMOND (Version: v0.8.31) was used to map the DEGs to the PHI-base database (Version: v4.1) to detect the fungal pathogenic genes. It was based on the query coverage and identity requirement [30-33].

RESULTS

Sequencing data filtering and de novo assembly of *R. solani* AG2-2IIIB transcriptome

BIn this study, six RNA libraries prepared each from sclerotia and mycelia of *R. solani* AG2-2IIIB, were sequenced. Subsequently, filtered out the excess adaptors and low-quality reads, a total of 67.47 and 68.83 million reads were obtained from sclerotia and mycelia, respectively. The average clean reads of Q20 percentage of sclerotia and mycelia was 96.80% and 96.82%, respectively. Average Q30 of Sclerotia and Mycelia was 88.92% and 88.77%. An average clean read ratio in sclerotia and mycelia was 87.48% and 89.25%, respectively (Table 1, Figure 1 A and 1B). These results showed that the data quality of the transcriptome was high and suitable for transcriptome analysis.

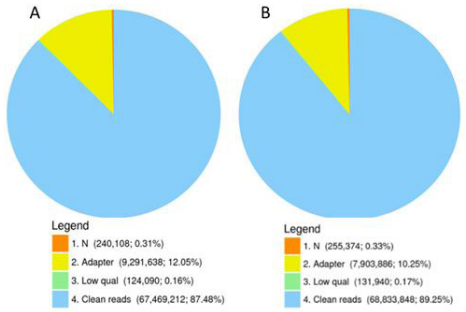

Figure 1) *Filter composition of raw data A. sclerotia (representative), B. Mycelia (representative)*
N: The total amount of reads which contain more than 5% unknown N base; Adaptor: The total amount of reads which contain adaptors; Low quality: More than 20% of bases in the total read have quality score lower than 15; Clean reads: Reads filtered with N reads, reads have adaptors and low-quality reads.

TABLE 1
Clean reads quality metrics.

Parameter/Sample mean	Sclerotia	Mycelia
Total mean Raw Reads (M)	77.13	77.13
Total mean clean Reads (M)	67.47	68.83
Total mean clean bases (Gb)	10.12	10.33
Clean Reads Q20 (%)	96.80	96.82
Clean Reads Q30 (%)	88.92	88.77
Clean Reads Ratio (%)	87.48	89.25
Total mean mapping ratio	51.00%	53.00%
Uniquely mapping ratio	6.51%	24.10%
Total mean gene number	9,839	10,718
Total mean transcript number	9,839	10,718

Genome mapping

After reads filtering, clean reads were mapped to reference genome using HISAT2. Total mean mapping ratio in sclerotia and mycelia were 51% and 53%, respectively. On average 52.00% reads were mapped, and the uniformity of the mapping result for each sample suggests that the samples were comparable. The mapping details were shown as Table 1.

Novel transcripts prediction

After genome mapping, StringTie was used to reconstruct transcripts, and with genome annotation information we identify novel transcripts by using Cuffcompare (a tool of Cufflinks) and predict the coding ability of those new transcripts using CPC. In total, we identify 6,063 novel transcripts, the detailed information is shown as Table 2.

SNP and INDEL detection

After genome mapping, we use GATK\[7\] to call single nucleotide polymorphism (SNP) and insertion/deletion (INDEL) variant for each sample. The SNP summary was shown as Table 3, and distribution of SNP and INDEL (Figure 2).

Correlation between samples

In order to reflect the gene expression correlation between samples, we calculated the Pearson correlation coefficients for all gene expression levels between each two samples and reflected these coefficients in the form of heat maps, shown as (Figure 3). The X and Y axis represent each sample. The color represents the correlation coefficient (the darker the color, the higher the correlation, the lighter the color, the lower the correlation).

The distribution of gene expression

The density map showed the change of gene abundance and reflected the concentration of gene expression in the sample interval, as show in (Figure 4). To show the gene amount under different FPKM value, we calculate the gene amount under three different FPKM ranges, FPKM ≤ 1, FPKM 1~10, FPKM ≥ 10, shown as (Figure 4).

Gene expression between samples and between groups

Venn diagram was used to illustrate expressed gene between two different samples shown as (Figure 5). The venn diagram showed 9706 overlapping genes in both mycelia and sclerotia. Only 133 non-overlapping genes were shared in the developmental process of sclerotia while 1012 genes were exclusively expressed in mycelia.

DEGs during sclerotia development of *R. solani* AG2-2IIIB

To determine the DEGs (Differentially expressed genes), the gene expression of sclerotia were compared to the mycelial stage. X axis represents log2 transformed fold change. Y axis represents -log10 (FDR-False Discovery Rate) transformed significance. Red points represent up-regulated DEGs which showed 2718 transcripts to be found in both samples. While blue points represent down-regulated DEGs (1313 transcripts) that were observed for the same. Gray points represent non-DEGs that represented 6820 genes (Figure 6).

Gene ontology analysis of DEG

A total of 4031 DEGs were categorized into 24 gene ontology (GO) terms under three major functional groups such as biological process, cellular component, and molecular biological function. The first group occupied biological process related genes included 29 cellular and 26 metabolic processed genes. Other genes were cellular localizations (10-genes), biogenesis (5-genes), detoxification (1-gene), nitrogen utilizations (1-gene) and signaling (1-gene). A high number of genes were engaged in cellular components processing such as cell as well as cell membrane, organelles, macromolecular complex, membrane-bounded lumen, and super molecular complex (Figure 7). The third group comprised with molecular function related genes: as seen in catalyzing (36-genes) and binding activity (28-genes), antioxidant (5-genes), structural molecular activity (5-genes), antioxidant and transport activity (2-genes each). The GO classification of up-regulated and down-regulated genes is shown in (Figure 8).

CAT, SOD, glutathione peroxidase, and putative protein disulfide-isomerase were classified in the antioxidant activity GO term, and SOD and CAT were predicted to be localized at the peroxisome.

TABLE 2
Summary of novel transcripts.

Total_Novel_Transcript	Coding_Transcript	Noncoding_Transcript	Novel Isoform	Novel Gene
6063	4204	1859	2978	1226

TABLE 3
SNP variant type summary.

Sample	A-G	C-T	Transition	A-C	A-T	C-G	G-T	Transversion	Total
Sclerotia	49,848	49,782	99,630	5,989	3,333	10,200	5,749	25,271	124,901
Mycelia	77,749	77,170	154,919	10,659	5,135	19,598	10,639	46,031	200,950

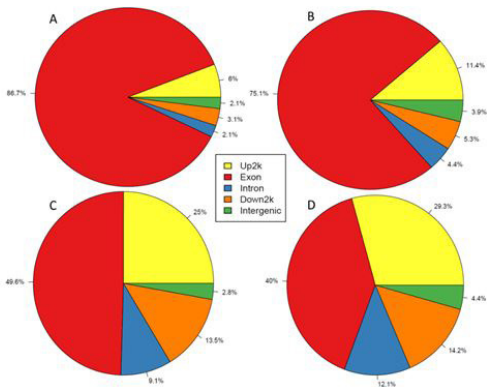

Figure 2) *Distribution of SNP and INDEL location. A. sclerotia, B. Mycelia, C. sclerotia, D. Mycelia. Up2k means upstream 2,000 bp area of a gene. Down2k means downstream 2,000 bp area of a gene.*

	RsS1	RsS2	RsS3	RsM1	RsM2	RsM3
RsS1	1	0.976	0.986	0.784	0.814	0.794
RsS2	0.976	1	0.966	0.782	0.775	0.786
RsS3	0.986	0.966	1	0.789	0.795	0.799
RsM1	0.784	0.782	0.789	1	0.954	0.952
RsM2	0.814	0.775	0.795	0.954	1	0.981
RsM3	0.794	0.786	0.799	0.952	0.981	1

Figure 3) *The X and Y axis represent each sample. The color represents the correlation coefficient (the darker the color, the higher the correlation, the lighter the color, the lower the correlation).*

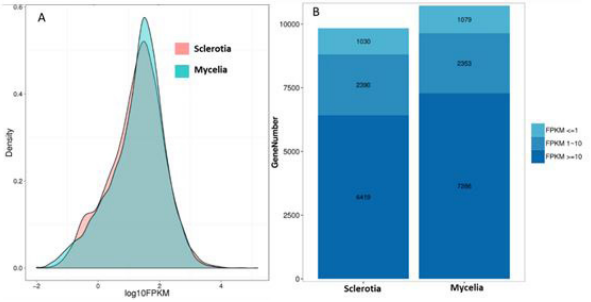

Figure 4) *Gene expression density map and distribution, A. gene expression density of sclerotia and mycelia, X axis represents the log10FPKM value. Y axis represents the gene density. B. Gene expression distribution in sclerotia and mycelia. X axis represents the sample name. Y axis represents the gene amount. The dark color means the high expression level which FPKM value >= 10, while the light color means the low expression level which FPKM value <= 1.*

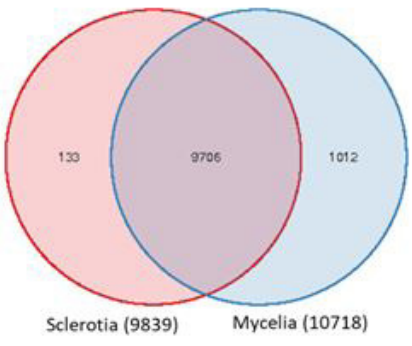

Figure 5) *The venn diagram illustrates of gene expression between samples.*

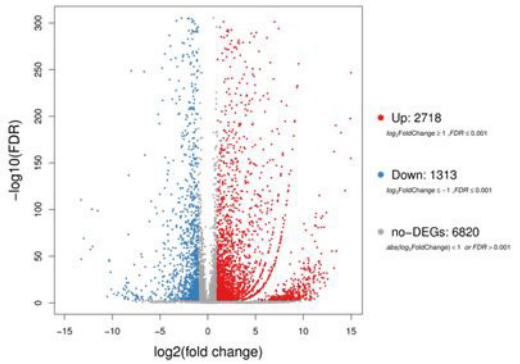

Figure 6) *Volcano plot displaying differential expressed genes between sclerotia and mycelia. The y-axis corresponds to the mean expression value of log 10 (p-value), and the x-axis displays the log2 fold change value. The red dots represent the up regulated expressed transcripts (p<0.05, false discovery rate (FDR) q<0.05) between sclerotia and mycelia; the green dots represent the transcripts whose expression down regulated (p<0.05, FDR q<0.05).*

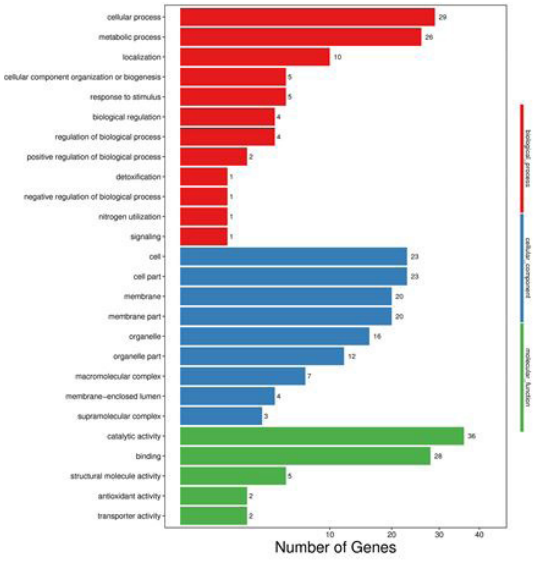

Figure 7) *GO classification of DEGs, which reflects in the biological process, cellular component, and molecular function. Different colors distinguish between biological processes ("red" column), cell component ("blue" column) and molecular function ("green" column). X axis represents number of DEG. Y axis represents GO term.*

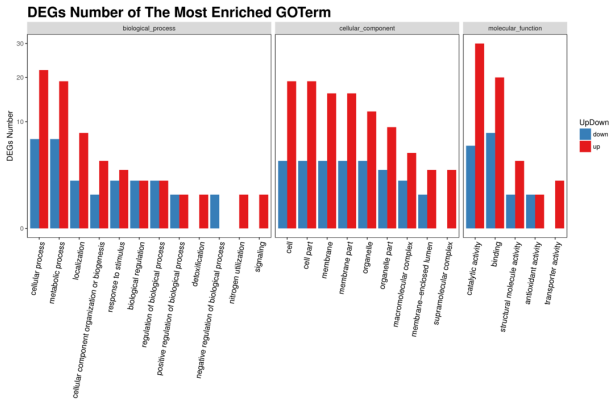

Figure 8) *GO classification of up-regulated and down-regulated genes.*

Pathway analysis of DEG

With DEGs, the kyoto encyclopedia of genes and genomes (KEGG) pathway classification and functional enrichment was performed. The pathway classification results are shown as (Figure 9), There were five branches out of seven KEGG pathways: Cellular Processes (293-genes), Environmental Information Processing (167-genes), Genetic Information Processing (344-genes), Metabolism (2,127 genes), and Organismal Systems (24-genes). Fungal cellular processes were involved with transport and catabolism, and cell growth and death related genes, while environmental information processing category included signal transduction and membrane transport genes. A moderately large number of transcripts were expressed and involved in the genetic information processing. Among them DNA-translation (130-gene), and DNA folding, sorting and degradation (105-gene), and replication and repair (62-gene), and transcription (47-gene) reprogramming genes were mostly abundant. A large number of genes found to play role in metabolic pathway as observed in global and overview maps (772-genes), carbohydrate (415-gene), amino acid (269-gene) and lipid (192-gene) metabolism. Fungal cellular processes were involved with 223 transport and catabolism, and 70 cell growth and death related genes.

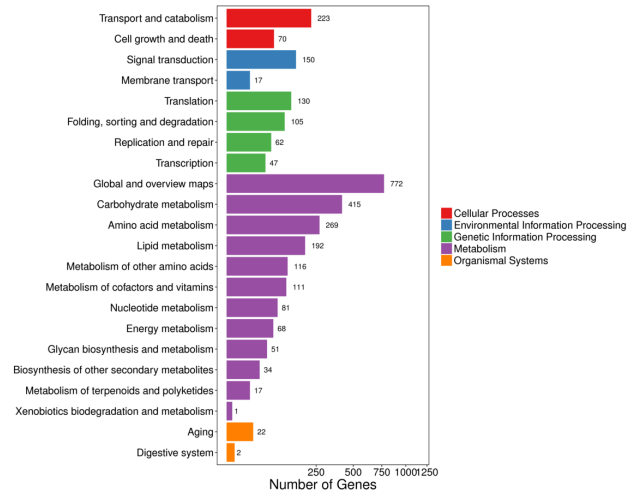

Figure 9) *Pathway classification of DEGs. X axis represents number of DEG. Y axis represents functional classification of KEGG.*

The KEGG pathway functional enrichment results were shown in (Figure 10). X axis represents enrichment factor. Y axis represents pathway name. The color indicates the q-value (high: dark blue, low: blue), the lower q-value indicates the more significant enrichment. Point size indicates DEG number (The bigger dots refer to larger amount). Rich Factor refers to the value of enrichment factor, which is the quotient of foreground value (the number of DEGs) and background value (total gene amount). The larger the value, the more significant enrichment.

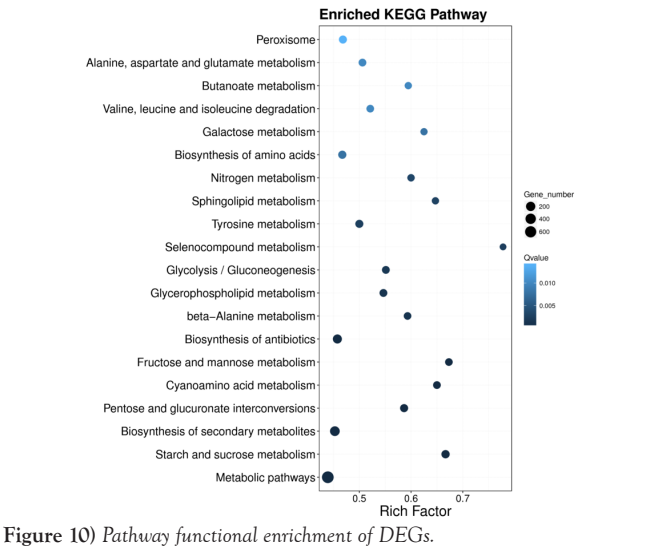

Figure 10) *Pathway functional enrichment of DEGs.*

In KEGG pathway showed less significant enrichment of peroxisome, alanine, asparate, Valine, leucine, isoleucine, glutamate, and butanoate metabolism. There was higher enrichment of metabolic pathways, biosynthesis of secondary metabolites and antibiotics, glycolysis/gluconeogenesis, glycerophospholipids, Tyrosine, sphingolipids, and selenocompounds. Moderate enrichment of the genes was reported in the following pathways included nitrogen metabolism, cyanoamino acid metabolism, β-Alanine, pentose and glucose interconversions.

Fungal pathogenic gene prediction

Based on the PHI database, we perform the fungal pathogenic gene prediction for all the DEGs, result shown as below: Toxins are one of the major molecules used by the necrotrophic fungi to dominate the host. These toxins can be proteins or secondary metabolites. In line with these previous findings, through RNA-seq analysis; cytochrome c oxidase, cytochrome c peroxidase, superoxide dismutase (SOD), cytochrome P450, oxidoreductase, signal peptidase complex, apoptosis-inducing factors, NADPH oxidase, chitinases, serine/threonine kinases, programmed cell death proteins, Transcription elongation factor 1-beta, subtilisin-like protease 8, poly-ubiquitin-A, glutathione peroxidase, phosphatidylserine decarboxylases, and hypothetical proteins were identified in the transcriptome of sclerotia and mycelia.

DISCUSSION

R. solani is one of the complex fungal pathogens that cause substantial economic loss to wide range of crops. Among the anastomosis subgroups, AG2-2IIIB known to be more aggressive to infect sugar beet than to AG2-2IV. AG2-2IIIB overwinters in crop residues and soil as sclerotia [9,34-36]. These sclerotia germinate under favorable condition to infect future sugar beet crops. Thus, sclerotia contribute pivotal role in the life cycle of *R. solani* AG2-2IIIB. Previously, the draft genome (56.02 Mb) analysis of the sugar beet pathogen *R. solani* AG2-2IIIB revealed presence of high number in secreted proteins and cell wall degrading enzymes such as polysaccharide lyases, glycoside hydrolase and carbohydrate esterase [37]. In order to unveil the molecular and genetic basis of sclerotia formation, here we analyzed the transcriptomic profile of mycelia and sclerotia.

The average mapping ratio to the draft genome of *Rhizoctonia solani* AG2-2IIIB was 51.00%, the average mapping ratio with gene was 50.39%; 12,077 genes were identified in which 10,851 of them are known genes and 1,226 of them were novel genes. 6,063 novel transcripts were identified in which 2,978 of them were previously unknown splicing event for known genes, 1,226 of them were novel coding transcripts without any known features, and the remaining 1,859 were long noncoding RNA. Overall, 133 and 1012 genes were exclusively detected in the sclerotia and mycelial sample, respectively. The total number of DEGs was 9706 in both samples. Other research on *R. solani* AG1 IA transcriptomics demonstrated a total of 5016 genes to be differentially expressed between sclerotia and mycelia. Among these genes, only 12 DEGs were verified following the reverse transcription quantitative PCR. Several genes reported to be highly upregulated during the sclerotia formation included superoxide dismutase (SOD), NADPH oxidase 1 (NOX1), and catalase (CAT) [17]. These studies demonstrated that SOD and CAT regulates the reactive oxygen species (ROS) generation and cellular homoeostasis in sclerotia development [17]. In this present study, a total number of upregulated and downregulated genes were 2718 and 1313, respectively. There was none differentially expressed genes cluster which was 6820. The up-regulates genes in sclerotia were, melanin biosynthesis genes (polyketide synthetase, Laccase-1, tyrosainase, polyketide cyclase), superoxide dismutase (SOD), ubiquitin family proteins, NADPH dehydrogenase, Peroxisomal ATPase, Glutathione S-transferase, endoglucanase-7, cytochrome 450, serine/threonine protein kinase (STPKs), GTPase activating protein, and a large group of hypothetical protein. These findings suggested pivotal role of these genes to regulate sclerotia formation of *R. solani* AG2-2IIIB.

GO classification of DEGs demonstrated the number of genes that are involved in the biological process, cellular component, and molecular function. The most abundant number of genes was involved in catalytic and binding activity (64 genes) which was followed by cellular and metabolic process (55 genes). The moderate number of genes was demonstrated to be involved in cellular localization and component organization (cell membrane, and organelles) or biogenesis (15 genes), response to stimuli (5 genes),

regulation of biological process (macromolecular or supramolecular complex) (5-genes), and structural molecular activity (5-genes). The least number of genes was demonstrated to be involved in detoxification, nitrogen utilization, antioxidant and transporter activity. Other research group demonstrated that carbohydrate metabolism to be upregulated during sclerotia maturation of *R. solani* AG-1. In addition, macromolecular or supramolecular complex and structural molecular activity found to be escalated. Several antioxidants enzymes to be differentially expressed in sclerotia included SOD, cytochrome C peroxidase, α-ketoglutarate dependent taurine dioxygenase, and dihydropteroate synthase [19]. Our study demonstrated a large group of genes to be involved in the development of sclerotia.

KEGG pathways further demonstrated functional enrichment of DEGs. There was less significant enrichment of peroxisome, alanine, asparate, valine, leucine, isoleucine, glutamate, and butanoate metabolism. This suggests that biosynthesis certain amino acids (Alanine, Aspartate, Glutamate), and degradation of other amino acids (Valine, Leucine, Isoleucine), antioxidants (ascorbic acid, glutathione) and enzymes (SOD, CAT) can alter the balance of reactive oxygen species and may affect sclerotial formation.

The top 20 genes from each category were selected, indicating that chitin synthase, NADPH dehydrogenase, NADPH oxidase 1 (NOX1), SOD, cytochrome P450, oxygendependent, choline dehydrogenase, O methylsterigmatocystin oxidoreductase, CAT, and NADPH-P450 reductase play particularly important roles in sclerotial formation. Further validate these genes function reverse genetics approach was adopted. Mutant progeny of RsNOX1 and RsNOX2 to be produced a smaller number of sclerotia and reduced phyto-pathogenicity. These findings suggested that NOX gene might be involved in ROS production and pathogenicity, as described by other research group in *S. sclerotiorum* [38,39].

CONCLUSION

We observed similar results with others silence mutant of the following genes; SOD, cytochrome P450, oxygendependent, choline dehydrogenase, O methylsterigmatocystin oxidoreductase, CAT, and NADPH-P450 reductase. These genes identified from this study revealed that polygenes to be involved in the development of sclerotia, thus this study provides useful information and possible targets for managing sclerotia mediated pathogenicity of *R. solani* AG2-2IIIB in sugar beet.

REFERENCES

1. Christou T. Penetration and host-parasite relationships of rhizoctonia-solani in bean plant. J Phytopathol. 1962;52:381.
2. Armentrout VN, Downer AJ. Infection cushion development by rhizoctonia-solani on cotton. J Phytopathol. 1987;77:619-23.
3. Lee DH, Choe YY, Lee JH, et al. Identification and pathogenicity of rhizoctonia species isolated from turfgrasses. Kor J Mycol, 1995;23:257-65.
4. Herr LJ. Sugar beet diseases incited by rhizoctonia spp. Rhizoctonia species: taxonomy, molecular biology, ecology, pathology and disease control. 1996;32:341-49.
5. Lee YS, Choi HS, Kim KS, et al. Analyses of genetic relationships of *rhizoctonia solani* isolates from various crop species and rapid identification of anastomosis groups with RAPD method. Kor J Mycol. 1998;26:373-379.
6. Parmeter JR, Sherwood RT, Platt WD, et al. Anastomosis grouping among isolates of thanatephorus cucumeris. J Phytopathol. 1969;59:1270.
7. Carling DE, Kuninaga S, Brainard KA, et al. Hyphal anastomosis reactions, rDNA-internal transcribed spacer sequences, and virulence levels among subsets of *Rhizoctonia solani* anastomosis group-2 (AG-2) and AG-BI. Phytopathology. 2002;92:43-50.
8. Sharon M, Kuninaga S, Hyakumachi M, et al. Classification of Rhizoctonia spp. using rDNA-ITS sequence analysis supports the genetic basis of the classical anastomosis grouping. Mycosci. 2008;49:93-114.
9. Sherwood RT. Anastomosis in relation to morphology and physiology of *rhizoctonia solani*. Phytopathol. 1967;57:830.
10. Windels CE, Nabben DJ. Characterization and pathogenicity of anastomosis groups of rhizoctonia-solani isolated from beta-vulgaris. J Phytopathol. 1989;79:83-88.
11. Willetts HJ, Bullock S. Developmental biology of sclerotia. Mycol Res. 1992;96:801-16.
12. Sumner DR. Sclerotia formation by Rhizoctonia species and their survival. Rhizoctonia species: taxonomy, molecular biology, ecology, pathology and disease control. 1996;23:207-15.
13. White JG. Effects Of temperature, light and aeration on production of microsclerotia by pyrenochaeta-lycopersici. Trans Bri Mycol Soc. 1976;67:497-498.
14. Ritchie F, Bain RA, McQuilken MP, et al. Effects of nutrient status, temperature and ph on mycelial growth, sclerotial production and germination of *rhizoctonia solani* from potato. J Plant Pathol. 2009;91:589-96.
15. Maurya S, Singh UP, Singh R, et al. Role Of air and light in sclerotial development and basidiospore formation in sclerotium rolfsii. J Plant Protection Res. 2010;50:206-09.
16. Lu L, Shu C, Liu C, et al. The impacts of natural antioxidants on sclerotial differentiation and development in *Rhizoctonia solani* AG-1 IA. Eur J Plant Pathol. 2016;146:729-740.
17. Liu B, Wang HD, Ma ZJ, et al. Transcriptomic evidence for involvement of reactive oxygen species in *Rhizoctonia solani* AG1 IA sclerotia maturation. Peerj. 2018;6.
18. Shu CW, Zhao M, Anderson JP, et al. Transcriptome analysis reveals molecular mechanisms of sclerotial development in the rice sheath blight pathogen *Rhizoctonia solani* AG1-IA. Funct Integrative Genomics. 2019;19:743-58.
19. Kwon YS, Kim SG, Chung WS, et al. Proteomic analysis of *rhizoctonia solani* AG-1 sclerotia maturation. Fungal Biol. 2014;118:433-43.
20. Cock PJA, Fields CJ, Goto N, et al. The sanger FASTQ file format for sequences with quality scores, and the solexa/illumina FASTQ variants. Nucleic Acids Res. 2010;38:1767-71.
21. Pertea M, Pertea GM, Antonescu CM, et al. StringTie enables improved reconstruction of a transcriptome from RNA-seq reads. Nature Biotechnol. 2015;33:290.
22. Kong L, Zhang Y, Ye ZQ, et al. CPC: Assess the protein-coding potential of transcripts using sequence features and support vector machine. Nucleic Acids Res. 2007;35:W345-W349.
23. Martin JA, Wang Z. Next-generation transcriptome assembly. Nature Rev Genet. 2011;12:671-82.
24. Trapnell C, Roberts A, Goff L, et al. Differential gene and transcript expression analysis of RNA-seq experiments with TopHat and cufflinks (vol 7, pg 562, 2012). Nature Protocols. 2014;9:2513.
25. Kim D, Landmead B, Salzberg SL, et al. HISAT: A fast spliced aligner with low memory requirements. Nature Methods. 2015;12:357-U121.
26. McKenna A, Hanna M, Banks E, et al. The Genome analysis toolkit: A mapreduce framework for analyzing next-generation DNA sequencing data. Genome Res. 2010;20:1297-303.
27. Li B, Dewey CN. RSEM: Accurate transcript quantification from RNA-Seq data with or without a reference genome. Bmc Bioinform. 2011;12.
28. Langmead B, Salzberg SL. Fast gapped-read alignment with Bowtie 2. Nature Methods. 2012;9:357-U354.
29. Audic S, Claverie JM. The significance of digital gene expression profiles. Genome Res. 1997;7:986-95.
30. Buchfink B, Xie C, Huson DH, et al. Fast and sensitive protein alignment using DIAMOND. Nature Methods. 2015;12:59-60.
31. Altschul SF, Gish W, Miller W, et al. Basic local alignment search tool. J Mol Biol. 1990;215:403-10.
32. Winnenburg R, Baldwin TK, Urban M, et al. PHI-base: A new database for pathogen host interactions. Nucleic Acids Res. 2006;34:D459-64.
33. Verma S, Gazara RK, Nizam S, et al. Draft genome sequencing and secretome analysis of fungal phytopathogen ascochyta rabiei provides insight into the necrotrophic effector repertoire. Scient Repo. 2016;6.
34. Schneider JHM, Schilder MT, Dijst G, et al. Characterization of *rhizoctonia solani* AG 2 isolates causing bare patch in held grown tulips in the Netherlands. Eur J Plant Pathol. 1997;103:265-79.

35. Yassin MA. Interaction of *rhizoctonia solani* anastomosis groups and sugar beet cultivars. J Pure App Microbiol. 2013;7:1869-76.

36. Zhao C, Li YT, Wu SY, et al. Anastomosis group and pathogenicity of Rhizoctonia spp. Associated with seedling damping-off of sugar beet in China. European J Plant Pathol. 2019;153:869-78.

37. Wibberg D, Andersson L, Tzelepis G, et al. Genome analysis of the sugar beet pathogen *Rhizoctonia solani* AG2-2IIIB revealed high numbers in secreted proteins and cell wall degrading enzymes. BMC Genomics. 2016;17:245.

38. Kim HJ, Chen C, Kabbage M, et al. Identification and characterization of sclerotinia sclerotiorum nadph oxidases. App Env Microbiol. 2011;77:7721-29.

39. Veluchamy S, Williams B, Kim K, et al. The CuZn superoxide dismutase from Sclerotinia sclerotiorum is involved with oxidative stress tolerance, virulence, and oxalate production. Physiol Mol Plant Pathol, 2012;78:14-23.